ESC European Society of Cardiology

Europace (2020) **22**, 1431–1441
doi:10.1093/europace/euaa111

BASIC SCIENCE

Repolarization instability and arrhythmia by I_{Kr} block in single human-induced pluripotent stem cell-derived cardiomyocytes and 2D monolayers

Cristina Altrocchi [1], Tessa de Korte[2,3†], Joyce Bernardi[1†], Roel L.H.M.G. Spätjens[1], Stefan R. Braam[2], Jordi Heijman[1], Antonio Zaza [4], and Paul G.A. Volders [1*]

[1]Department of Cardiology, CARIM, Maastricht University Medical Center+, PO Box 5800, 6202 AZ Maastricht, The Netherlands; [2]Ncardia, Leiden 2333 BD, The Netherlands; [3]Department of Anatomy and Embryology, Leiden University Medical Center, 2333 ZD Leiden, The Netherlands; and [4]Laboratory of Cardiac Cellular Physiology, Department of Biotechnology and Bioscience, University of Milano-Bicocca, Milan, Italy

Received 31 October 2019; editorial decision 15 April 2020; accepted after revision 18 April 2020; online publish-ahead-of-print 8 August 2020

Aims Human-induced pluripotent stem cell-derived cardiomyocytes (hiPSC-CMs) have proven valuable for studies in drug discovery and safety, although limitations regarding their structural and electrophysiological characteristics persist. In this study, we investigated the electrophysiological properties of Pluricyte® CMs, a commercially available hiPSC-CMs line with a ventricular phenotype, and assessed arrhythmia incidence by I_{Kr} block at the single-cell and 2D monolayer level.

Methods and results Action potentials were measured at different pacing frequencies, using dynamic clamp. Through voltage-clamp experiments, we determined the properties of I_{Na}, I_{Kr}, and I_{CaL}. Intracellular Ca^{2+} measurements included Ca^{2+}-transients at baseline and during caffeine perfusion. Effects of I_{Kr} block were assessed in single hiPSC-CMs and 2D monolayers (multi-electrode arrays). Action-potential duration (APD) and its rate dependence in Pluricyte® CMs were comparable to those reported for native human CMs. I_{Na}, I_{Kr}, and I_{CaL} revealed amplitudes, kinetics, and voltage dependence of activation/inactivation similar to other hiPSC-CM lines and, to some extent, to native CMs. Near-physiological Ca^{2+}-induced Ca^{2+} release, response to caffeine and excitation–contraction coupling gain characterized the cellular Ca^{2+}-handling. Dofetilide prolonged the APD and field-potential duration, and induced early afterdepolarizations. Beat-to-beat variability of repolarization duration increased significantly before the first arrhythmic events in single Pluricyte® CMs and 2D monolayers, and predicted pending arrhythmias better than action-potential prolongation.

Conclusion Taking their ion-current characteristics and Ca^{2+} handling into account, Pluricyte® CMs are suitable for *in vitro* studies on action potentials and field potentials. Beat-to-beat variability of repolarization duration proved useful to evaluate the dynamics of repolarization instability and demonstrated its significance as proarrhythmic marker in hiPSC-CMs during I_{Kr} block.

Keywords Human-induced pluripotent stem cell-derived cardiomyocytes • Ion channel • Calcium handling • Beat-to-beat variability of repolarization • Arrhythmia inducibility • Multi-electrode arrays

* Corresponding author. Tel: +31 43 3875106; fax: +31 43 3875104. *E-mail address*: p.volders@maastrichtuniversity.nl

† These authors contributed equally to the study.

What's new?

- We took a multilevel approach (patch clamp and multi-electrode array) to examine electrophysiological characteristics and the effects of I_{Kr} block in a commercially available human-induced pluripotent stem cell-derived cardiomyocyte (hiPSC-CM) line with a ventricular-like phenotype.
- For the first time in single hiPSC-CMs and 2D monolayers, the temporal changes in beat-to-beat variability of repolarization duration were assessed.
- Beat-to-beat variability of repolarization duration was superior to action-potential prolongation *per se* in predicting arrhythmic events during I_{Kr} block.

Introduction

Human-induced pluripotent stem cell-derived cardiomyocytes (hiPSC-CMs) have created new perspectives in many fields, including developmental biology, drug testing, safety pharmacology, and disease modelling.[1] The implementation of cellular models for *in vitro* safety pharmacology has reduced drug attrition due to proarrhythmic effects.[2] Concurrently, the approval rate of new drugs fell,[3] indicating the need for more specific proarrhythmic tests and biomarkers. In this context, a public–private collaboration, the CiPA (*C*omprehensive *I*n vitro *P*roarrhythmia *A*ssay) initiative, proposed the use of hiPSC-CMs to detect missed or unanticipated electrophysiological responses to medicinal compounds and assess proarrhythmic risk.[4]

Although protocols for reprogramming, differentiation and maturation of hiPSC-CMs have improved over the last decade, structural and electrophysiological limitations hinder their wide-spread application. hiPSC-CMs have a poorly developed T-tubular system, so that Ca^{2+} handling only partially resembles that of human adult native cardiomyocytes.[5] Furthermore, the maximum diastolic potential of hiPSC-CMs is generally less hyperpolarized than that of adult myocytes, which could be explained by a higher expression of HCN4 channels and a smaller inward-rectifier K^+ current (I_{K1}).[6] Nonetheless, the use of hiPSC-CMs is growing, and various groups and companies have developed cell lines with more mature phenotypes, which are potentially suitable for drug screening.

In the present study, we investigated the electrophysiological and Ca^{2+}-handling properties of one such hiPSC-CMs cell line, commercially available as Pluricyte® Cardiomyocytes (Pluricyte® CMs). The injection of a simulated virtual I_{K1} through the dynamic-clamp technique (DC) allowed us to restore a physiological resting membrane potential, and to determine the rate dependence of the evoked action potentials (APs). Furthermore, we showed that the biophysical properties of crucial currents that characterize these APs (i.e. I_{Na}, I_{CaL}, I_{Kr}) and Ca^{2+}-handling properties are similar to other sources of hiPSC-CMs and, in some cases, comparable to native CMs. We determined the potential value of hiPSC-CMs for proarrhythmic risk assessment using repolarization prolongation, beat-to-beat variability of repolarization duration (BVR), and arrhythmia incidence as indicators. We demonstrate that, along with repolarization prolongation, BVR increases after application of the I_{Kr} blocker dofetilide, both in single hiPSC-CMs and 2D monolayers. We also showed, for the first time in hiPSC-CMs, that an excessive increase in BVR precedes the first arrhythmic events during I_{Kr} block and therefore predicts the occurrence of arrhythmic events better than AP-prolongation *per se*.

Methods

Cell culture

hiPSC-CMs (Pluricyte® CMs) were provided by Ncardia (Gosselies, Belgium) as cryopreserved samples, and stored in liquid nitrogen until thawed. Thawing and culturing were carried out according to the manufacturer's protocols. Once thawed, Pluricyte® CMs were maintained in an incubator (37°C, 5% CO_2), in Pluricyte® Cardiomyocyte Medium (Ncardia). Medium was refreshed at day 1 post-thaw and subsequently every other day. For manual patch clamp, the cells were seeded on 6-mm glass coverslips (VWR, Radnor, USA) coated with Matrigel (Corning Inc., New York, USA, Ref. 354277) and placed into 35-mm dishes (Greiner Bio-One, GmbH, Solingen, Germany), with a density of 300 000–400 000 cells/dish. For patch clamp, Pluricyte® CMs were tested 5–7 days after thawing. A single coverslip was placed in the recording chamber of an inverted microscope and used for about 1 h of recordings. For multi-electrode arrays (MEA), cells were seeded onto 48-well MEA plates (Axion Biosystems, Inc., Atlanta, USA) coated with fibronectin (50 µg/mL in PBS with Ca^{2+} and Mg^{2+}, Sigma-Aldrich, Cat. No. F-1141), with a density of 30 000 cells/well. Multi-electrode array recordings were performed at day 8 post-thaw.

Single-cell measurements (patch clamp)

Patch-clamp experiments were performed using an inverted microscope (Nikon Inc., Tokyo, Japan), with an Axon 200B amplifier (Molecular Devices, LLC, San Jose, USA) and an Axon Digidata 1322a digitizer (Molecular Devices, LLC, San Jose, USA). Data were acquired using pCLAMP8 (Molecular Devices, LLC, San Jose, USA) and analysed with Clampfit 10.7 (Molecular Devices, LLC, San Jose, USA). Extracellular and pipette solutions for each condition are summarized in the Supplementary material online, *Table S1*, in which the protocols used in voltage-clamp experiments are also shown (Supplementary material online, *Figure S1*).

I_{Na} recordings were performed at room temperature (22 ± 1°C). Currents were sampled at 20 kHz after low-pass filtering at 10 kHz. The protocol repetition rate was 0.2 Hz. The holding potential was set to −70 mV and a 200 ms-conditioning step at −120 mV assured complete recruitment of Na^+ channels (Supplementary material online, *Figure S1A*). This protocol allowed the simultaneous recording of steady-state activation (in the increasing voltage steps of 500 ms) and inactivation in the final step at −20 mV for 25 ms. For steady-state activation, the voltage dependence of normalized Na^+ conductance [g/g_{max}; with g calculated as $I/(V - E_{rev})$, where I is the peak I_{Na} during a depolarizing step, V is the command potential, and E_{rev} is the reversal potential of I_{Na}] was fitted with a Boltzmann equation [$g/g_{max} = 1/[1 - \exp(V - V_{1/2})/k]$] to determine the membrane potential for half-maximal activation ($V_{1/2}$) and the slope factor (k). The same equation was applied to determine $V_{1/2}$ and k for steady-state inactivation using I/maximal I (I_{max}) at the −20 mV final step. The intersection of the steady-state voltage-dependent activation and inactivation ('window current') was analysed to deduct the voltage range, the 'crossing point' and the maximum amplitude reached at that point in voltage (in arbitrary units). The time course of inactivation was fitted using a double exponential function [$I(t)$=A1*exp(-t/τ1)+A2*exp (-t/τ2)], where A is amplitude and τ time constant. Borosilicate glass pipettes (Science Products GmbH, Germany) were pulled (DMZ Universal

Electrode Puller, Zeitz-Instruments, GmbH Martinsried, Germany) at a resistance of 1.5–2.5 MΩ.

I_{Kr} was recorded at 36 ± 1°C as the current sensitive to its selective blocker dofetilide. Five μmol/L nifedipine and 1 μmol/L HMR1556 were added to further rule out interference by I_{CaL} and I_{Ks}, respectively. From a holding potential of −40 mV, voltage steps (from −60 to +50 mV) of 1 s were applied (protocols repetition rate was 0.3 Hz, Supplementary material online, *Figure S1*). I_{Kr} amplitude was measured as the peak tail current upon repolarizing to the holding potential. The activation curve was obtained from the tail I_{Kr} *I/V* relationship fitted with the Boltzmann function to determine voltage of half-maximal activation ($V_{1/2}$, mV) and slope factor (*k*, mV). The 'rectifier ratio' was calculated as the ratio between the conductance (G) of the current at the end of the depolarizing steps and the correspondent tail conductance (at −40 mV). The time course of current deactivation was analysed using a single-exponential function, yielding a time constant (τ).

I_{CaL} recordings were performed at room temperature, to minimize current run-down. Currents were sampled at 10 kHz after low-pass filtering at 5 kHz; the protocol's repetition rate was 0.2 Hz. Steady-state activation was assessed in 200 ms-long voltage steps (from −60 to +60 mV), preceded by a 200 ms-step to −40 mV to fully inactivate I_{Na} (Supplementary material online, *Figure S1*). Steady-state inactivation was analysed in the final 300 ms-step at 0 mV, preceded by increasing voltage steps of 2 s from −60 to +5 mV. The holding potential was, in both cases, −70 mV. Steady-state activation and inactivation were fitted using a Boltzmann equation, as reported for I_{Na}. Window-current analysis was carried out as for I_{Na}. The time course of inactivation was analysed using a mono-exponential function and assessing the time constant (τ). Intracellular Ca^{2+} was buffered by adding 10 mmol/L ethylene glycol-bis(β-aminoethyl ether)-N, N, N′,N′-tetraacetic acid (EGTA) to the intracellular solution (Supplementary material online, *Table S1*).

Current clamp: Contracting Pluricyte® CMs were selected for AP recordings at 36 ± 1°C, using the perforated patch-clamp technique (Supplementary material online, *Table S1*). Pluricyte® CMs were paced to steady-state at frequencies of 0.5, 1, 2 and 3 Hz. No correction of the liquid junction potential was made.

Dynamic clamp: In hiPSC-CMs, DC was used to overcome the lower expression of I_{K1}, by injecting I_{K1} from a human ventricular numerical model into the patched cells (details in the Supplementary material online, *Methods*).

Intracellular Ca^{2+} recordings

Before recordings, Pluricyte® CMs were incubated for 20 min in the membrane-permeable Ca^{2+}-sensitive dye Fluo4-AM (5 μmol/L) and then washed for 5–10 min with Tyrode to eliminate the dye excess. The dye was excited at 480 nm and emission was collected through a 535-nm band-pass filter using a photomultiplier detection system (Photon Technology International, Inc., NJ, USA). Light emission was amplified, converted to voltage, low-pass filtered and digitized at 2 kHz. Background luminescence was recorded from a cell-free field and subtracted. The fluorescence signal of diastolic Ca^{2+} of the first recorded transient was used as reference fluorescence (F_0) for signal normalization (F/F_0). Intracellular Ca^{2+} recordings were performed under voltage-clamp conditions, at 36 ± 1°C.

From a holding potential of −40 mV, depolarizing steps of 200 ms to 0 mV were applied to trigger Ca^{2+}-transients; the total sweep duration was 3 s. To quantify sarcoplasmic-reticulum (SR) Ca^{2+} content, a caffeine pulse (10 mmol/L) was applied after a loading train of three depolarizing steps and the amplitude of the resulting Ca^{2+}-transient was measured. To analyse the rate of Ca^{2+}-transient relaxation, a standard mono-exponential function was used to fit the decay of the depolarization-induced Ca^{2+}-transient, yielding a time constant τ. The fractional release was calculated as the ratio between the amplitude of depolarization-induced Ca^{2+}-transient and SR Ca^{2+} content and, for clarity, converted to a percentage. The excitation–contraction coupling (ECC) gain was calculated as the ratio between the amplitude of depolarization-induced Ca^{2+} transient and peak amplitude of the corresponding I_{CaL} signal[7]; ECC gain was therefore expressed in arbitrary units (A.U.).

Multi-electrode arrays

At day 8 post-thaw, 2 h after medium refreshment, the 48-well MEA plate seeded with Pluricyte® CMs was placed in the Maestro MEA device (768-channel amplifier) with an integrated heating system, temperature controller and data-acquisition interface (Axion BioSystems, Inc., Atlanta, 94 USA). Baseline recordings were performed after an equilibration period of 10 min. Pluricyte® CMs were cumulatively exposed to four different concentrations of dofetilide (0–10 nmol/L, Tocris-BioTechne, Abingdon, UK) under non-sterile conditions in eight replicates for each concentration. Vehicle control was DMSO (0.000003–0.0003%; $n = 6$). Final DMSO concentrations matched the dofetilide final concentrations. Recordings of 10 min were performed after 20 min incubation time per concentration. All recording conditions were at 37°C using standard filters and amplifiers in spontaneous cardiac mode (12.5 Hz sampling frequency; 2 kHz Kaiser window; 0.1 Hz IIR). The field-potential detection threshold was set at 300 μV. To determine the effect of dofetilide on the field-potential duration (FPD) with high certainty, data files were analysed using the CiPA Tool software (Axion Biosystems, version 2.0.14). For each well, the FPD was quantified from the electrode with the best trackable repolarization feature ('golden electrode'). Markers for depolarization peak and repolarization peak were adjusted manually if needed.

Beat-to-beat variability of action-potential and field-potential duration

Action-potential duration (APD)-BVR was quantified as short-term variability of hiPSC-CMs APD at 90% repolarization (APD_{90}), for 30 consecutive APs, at baseline and during dofetilide application, before any early afterdepolarization (EAD) had occurred, using the following formula: $\sum|APD_{90(n-1)} - APD_{90(n)}|/(nAPs*\sqrt{2})$. In the cells that did not show EADs, we selected the interval at which the effect of the dofetilide was maximal. Repolarization delay *per se* was not considered an EAD unless the membrane potential showed a clear depolarization before complete repolarization.

FPD-BVR: per condition, 4 min on a total of 10 min MEA recording were exported for BVR analysis in Clampfit 11 using the Axion Data Export Tool (Axion Biosystems, version 3.2.5). Recordings were selected from one electrode per well, four wells per condition. The electrode corresponded to the same electrode used for FPD analysis by the CiPA Tool. The selection of the 30 consecutive beats was made by evaluating the RR interval variability and by selecting the moment with the smallest variation during the 4 min, to rule out any interference. If an arrhythmic event was detected, BVR was calculated in the 30 beats before the very first one. BVR was calculated using the same formula as described for the APD-BVR. In total, BVR at four conditions was analysed: baseline, 0.3 nmol/L, 1 nmol/L, and 3 nmol/L dofetilide.

Statistical analysis

Data are expressed as mean ± standard error of the mean. All statistical tests were conducted using SPSS (IBM, USA), and a *P*-value < 0.05 was considered significant. For the analysis of the single-hiPSC-CM experiments, a paired- or unpaired *T*-test was used, with a confidence interval level of 95%. When the data did not satisfy the assumptions of parametric tests (i.e. the samples were not normally distributed, such as the values of

BVR in the +EADs group), a non-parametric test was used (related samples Wilcoxon signed-rank test). For MEA data, repeated-measures analysis of variance with a confidence interval adjustment (Bonferroni) was used.

Results

Electrophysiological characterization of Pluricyte® CMs: action-potential features

In Pluricyte® CMs, the average maximum diastolic membrane potential was −47 ± 1.5 mV (n = 23). To reach a value of approximately −85 mV, a modelled, real-time computed I_{K1}-like current was injected.[8] *Figure 1A* shows a representative example of the DC approach: starting from a spontaneous series of APs, the injection of the computed I_{K1} restored the resting membrane potential to −85 mV and conferred the AP a typical adult-like shape. *Figure 1B* depicts a single AP from a Pluricyte® CM, with the correspondent current injected by DC.

Using DC, we measured the APD_{90} at different pacing lengths. In Pluricyte® CMs, APD_{90} adapted to increasing cycle length, as expected ($APD_{90\text{-}330ms}$: 138 ± 18, n = 7; $APD_{90\text{-}500ms}$: 166 ± 23 ms, n = 11; $APD_{90\text{-}1000ms}$: 184 ± 19 ms, n = 16; $APD_{90\text{-}2000ms}$: 193 ± 37 ms, n = 6). The relationship between these two parameters showed a non-linear trend (*Figure 1C*).

Ion currents and Ca^{2+} handling in Pluricyte® CMs

Na current (I_{Na})

I_{Na} in Pluricyte® CMs (*Figure 2A*) showed a peak amplitude of −201 ± 20 pA/pF at −21 ± 1 mV (n = 19; *Figure 2B*). The time course of inactivation was best fitted by a double exponential equation, generating a fast and a slow time constant (τ), as depicted in *Figure 2C*. At the voltage of maximum I_{Na} activation (−20 mV), the slow and fast components reached values of 16 ± 1 ms and 1.8 ± 0.1 ms, respectively (n = 16).

The steady-state activation and inactivation curves were fitted by the Boltzmann equation and the estimated midpoints ($V_{1/2}$) were −36.9 ± 1.0 and −78.7 ± 1.7 mV, respectively, with k values of 5.3 ± 0.2 and 7.2 ± 0.2 mV (*Figure 2D*, n = 19). The area under the intersection of the two curves, known as 'window' current, spanned voltages between −70 and −30 mV. A small, non-inactivating component was also present. The voltage at which the window current was maximal (5% of maximal conductance) was −57 mV (inset *Figure 2D*).

Rapidly-activating delayed-rectifier K^+ current I_{Kr}

A representative example of I_{Kr} recorded in Pluricyte® CMs is depicted in *Figure 2E*. The I–V plot of I_{Kr} tail shows a peak of 1.5 ± 0.1 pA/pF at +28 ± 4 mV (n = 18; *Figure 2F*). When the activation curve was fitted with the Boltzmann equation, the $V_{1/2}$ was

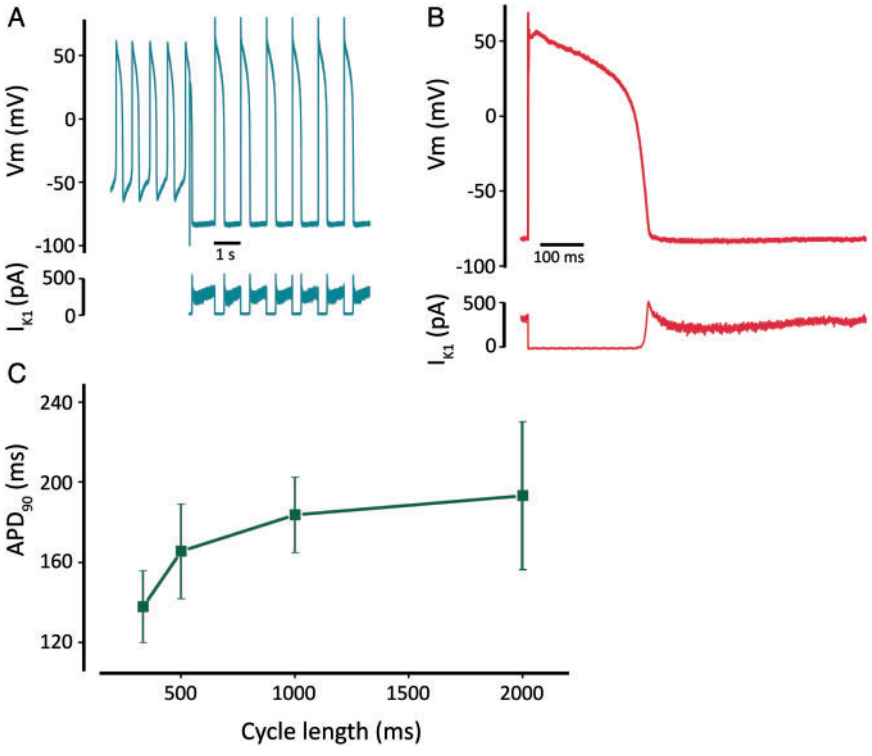

Figure 1 Action-potential characteristics of Pluricyte® CMs at baseline. (*A*) Series of spontaneous action potentials with pronounced diastolic depolarization. The injection of computed I_{K1} through dynamic clamp led to a resting membrane potential comparable to that of native CMs. (*B*) Zoom-in of action potential showing a typical native-like contour. The profile of the computed and injected I_{K1} is depicted below. (*C*) Rate dependence of action-potential duration (APD_{90}) (n = 7, 11, 16, 6 CMs for pacing cycle lengths of 333, 500, 1000, and 2000 ms).

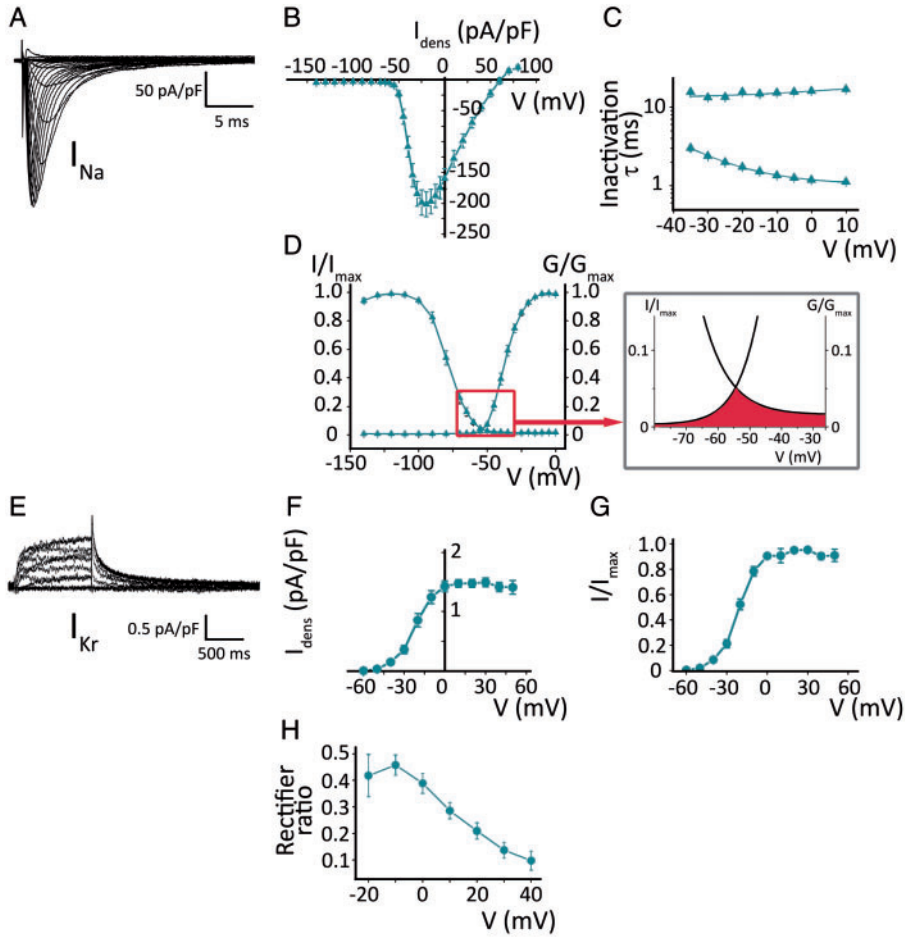

Figure 2 Ion currents in Pluricyte® CMs. (*A*) Voltage-dependent I_{Na} activation; representative family of traces. (*B*) I_{Na}-density I–V relationship ($n = 19$). (*C*) Kinetics of voltage-dependent steady-state inactivation, obtained by a double exponential fit. (*D*) Steady-state activation and inactivation, with conductance and current normalized to their maximum values. Inset shows the 'window-current', as the area under the crossing between the steady-state activation and inactivation curves. (*E*) Voltage-dependent I_{Kr} activation. (*F*) I_{Kr}-density I–V relationship ($n = 18$). (*G*) Steady-state activation of I_{Kr}; current normalized to maximum value. (*H*) Rectifier ratio, correlating the conductance of the depolarizing step with the I_{Kr}-tail conductance.

−21 ± 2 mV, with a *k* of 8.4 ± 0.8 mV (*Figure 2G*, $n = 18$). *Figure 2H* shows the relationship between the depolarizing step and the tail conductance, known as rectifier ratio, for each voltage. The time constant (τ) of tail current deactivation (at −40 mV), estimated by mono-exponential fitting, was 365 ± 19 ms ($n = 9$).

L-type Ca^{2+} current (I_{CaL})

Figure 3A shows a representative I_{CaL} recording in a Pluricyte® CM. During voltage-dependent activation, I_{CaL} reached a peak of −12 ± 1 pA/pF at 0 mV ($n = 14$; *Figure 3B*). I_{CaL} inactivation was fitted by a single-exponential equation and at 0 mV (maximum I_{CaL} density) the τ was 51.8 ± 4.5 ms (*Figure 3C*). The $V_{1/2}$ of the steady-state activation was −17.1 ± 1.0 mV and a slope factor (*k*) of 6.7 ± 0.2 mV ($n = 10$). The steady-state inactivation $V_{1/2}$ was −38.3 ± 1.2 mV, with a *k* of 5.8 ± 0.3 mV (*Figure 3D*, $n = 9$). Window I_{CaL} (inset of *Figure 3D*) showed a voltage range between −40 and −15 mV, and achieved 20% of maximal activation at −34 mV.

Ca^{2+} handling

Cells showed robust depolarization-triggered Ca^{2+}-transients, characterized by a time-to-peak of 194 ± 10 ms and a time constant of decay (τ) of 309 ± 23 ms (*Figure 3E*; $n = 23$). The triggering inward membrane current, measured simultaneously with the transients, mainly reflects I_{CaL}, with a peak density of −13.8 ± 1.9 pA/pF (at 0 mV; $n = 23$), comparable to I_{CaL} recorded at the same potential in the voltage-clamp experiments above. To quantify the efficiency of the coupling between the I_{CaL} and SR Ca^{2+} release, we calculated the ECC gain. At 0 mV, the ECC gain yielded a value of 0.14 A.U. ($n = 8$). It should be noted that, because of its arbitrary units, this value should be used only as a qualitative reference for comparisons.

In response to the caffeine pulse, Pluricyte® CMs generated Ca^{2+}-transients with a larger amplitude and longer duration compared to the preceding I_{CaL}-triggered transients (1.66 ± 0.22 vs. 0.87 ± 0.14 A.U., $P < 0.001$; *Figure 3F–G*; $n = 9$). Exponential fitting of the decay of the caffeine-induced transient, which is representative of Na^{+}-Ca^{2+}-exchange-dependent (SERCA-independent) Ca^{2+} clearance, yielded

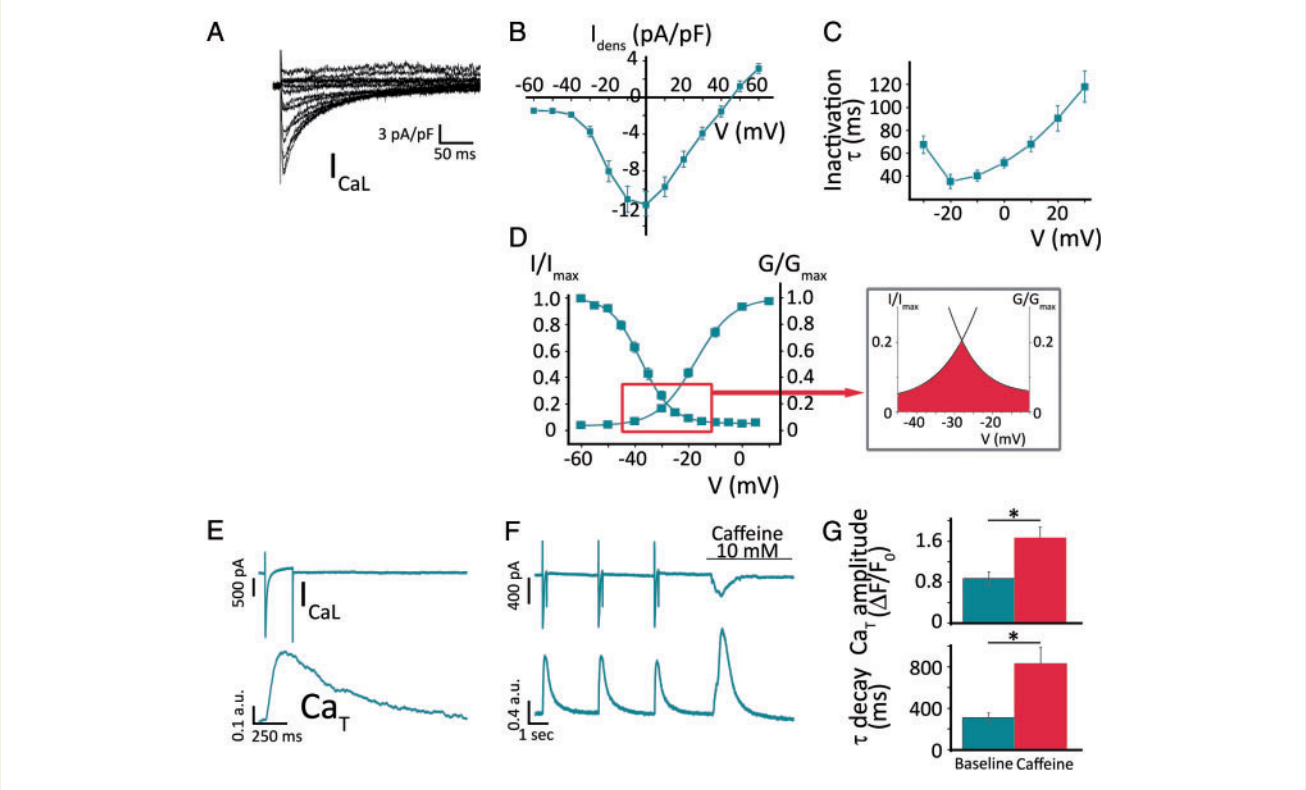

Figure 3 Ca^{2+} handling in Pluricyte® CMs. (*A*) Voltage-dependent I_{CaL} activation; representative family of traces. (*B*) I_{CaL}-density I–V relationship ($n = 14$). (*C*) Kinetics of inactivation of I_{CaL} (single exponential fit). (*D*) Steady-state activation and inactivation, fitted by Boltzmann equation. The inset depicts window I_{CaL}. (*E*) Simultaneous recordings of I_{CaL} and Ca^{2+}-transients (Ca_T) as a representative example. (*F*) Effect of caffeine (10 mmol/L) on membrane current and Ca_T, in a Pluricyte® CM. (*G*) Average values of CaT amplitude (above) and decay time constant (below), at baseline and during caffeine perfusion.

a time constant of 833 ± 158 ms. This value is much larger than the τ of depolarization-induced Ca^{2+}-transients (312 ± 44 ms; $n = 9$; $P = 0.003$; *Figure 3G*), thus suggesting a significant SERCA contribution to cytosolic Ca^{2+} clearance during physiological activity, quantified as 57 ± 0.1% ($n = 9$).

The fraction of total SR Ca^{2+} content released by the I_{CaL}-triggered Ca^{2+}-transient, known as 'fractional SR Ca^{2+} release', was 51 ± 4.7% ($n = 9$).

Caffeine elicited a transient inward current (I_{ti}), with a peak current density of −2.5 ± 0.4 pA/pF.

Repolarization effects by I_{Kr} block in single human-induced pluripotent stem cell-derived cardiomyocytes

We superfused the cells with dofetilide (100 nmol/L), a specific I_{Kr} blocker clinically linked to an increased *in vivo* risk of torsades de pointes (TdP),[4] while pacing them at 1 Hz. We evaluated three parameters: the prolongation of APD_{90}, the degree of BVR [a measure of repolarization (in)stability], and the occurrence of EADs. *Figure 4A* depicts the shortest and the longest APs (in a series of 30) before and during dofetilide treatment, with the Poincaré plot visualizing the beat-by-beat APD_{90} dynamics (*Figure 4B*). On average, the APD_{90} prolonged from 135 ± 10 ms at baseline to 227 ± 16 ms (in the absence of EADs; *Figure 4C*; $n = 20$; $P < 0.001$). Interestingly, BVR also increased from 2.7 ± 0.3 ms at baseline to 14.2 ± 2.5 ms during dofetilide treatment (*Figure 4D*; $n = 20$; $P < 0.001$). *Figure 4E* shows a representative example of a cell in which dofetilide caused an EAD. In 20 cells, none showed EADs at baseline, while 10 exhibited EADs during dofetilide and 10 did not (*Figure 4F*). For further analysis, we divided the dofetilide-treated cells in two groups, according to whether they (eventually) generated EADs ('+EADs'; $n = 10$) or not ('no EAD'; $n = 10$). *Figure 5A* depicts a representative example of a cell from the 'no EAD' group. Compared to baseline (trace), APD_{90} and BVR gradually increased (*Figure 5B*). Likewise, we analysed a cell from the '+EADs group' (*Figure 5C*). In this case, BVR excessively increased *before* the first EAD occurred, as shown in *Figure 5D*.

On average, dofetilide caused a significant APD increase in both groups (no-EAD group: APD_{bas} = 123 ± 13 ms vs. APD_{dof} = 205 ± 23 ms; $n = 10$; $P < 0.001$. +EADs group: APD_{bas} = 147 ± 16 ms vs. APD_{dof} = 248 ± 22 ms; $n = 10$; $P < 0.001$, *Figure 5E*). Interestingly, the APD after dofetilide treatment was not significantly different between the two groups ($APD_{dof\text{-}noEADs}$ = 205 ± 23 ms vs. $APD_{dof\text{-}+EADs}$ = 248 ± 22 ms; $n = 10$; 10; $P = 0.20$). The average BVR in the EAD-negative cells was ∼4-fold larger after dofetilide compared to baseline (no-EADs: BVR_{bas} = 2.3 ± 0.4 ms vs. BVR_{dof} = 8.3 ± 1.8 ms;

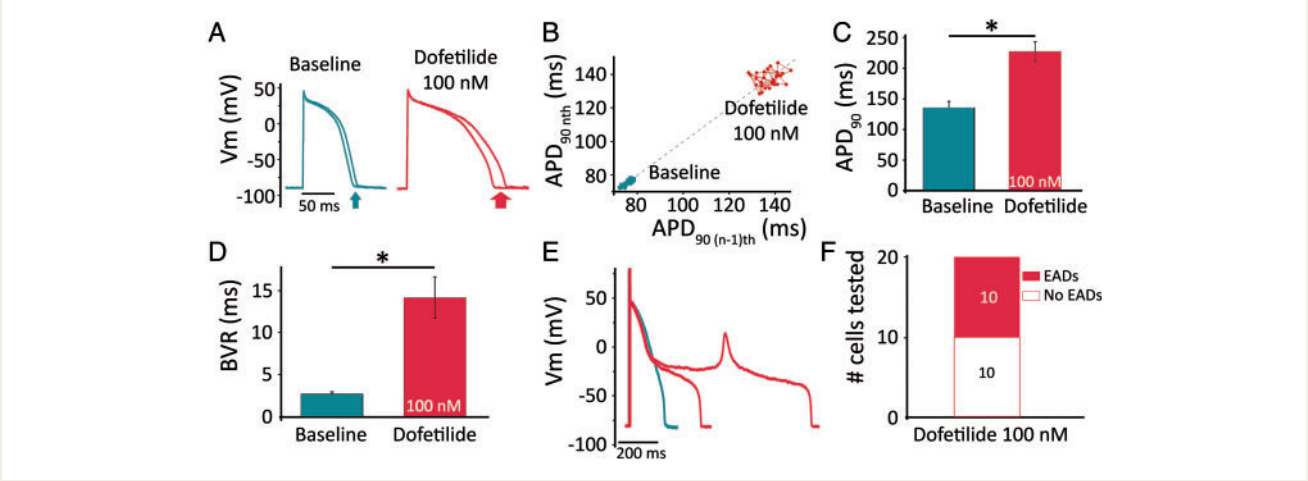

Figure 4 Action-potential effects of I_{Kr} block by dofetilide in Pluricyte CMs. (*A*) Repolarization variability visualized by the shortest and the longest APs with/without EADs in a series of 30 consecutive beats. (*B*) Poincaré plot of APD_{90} in a representative cell, showing increased BVR by dofetilide (in the absence of EADs). (*C*) Average increase in APD_{90} without EADs ($n = 20$). (*D*) Average increase in BVR at baseline and during dofetilide ($n = 20$). (*E*) Repolarization prolongation and EAD generation (red traces; 100 nmol/L dofetilide) in a representative cell. (*F*) Incidence of EADs in 20 cells treated with dofetilide.

$n = 10$; $P = 0.004$), while the +EAD group showed (before the first EAD) almost seven times larger BVR value than at baseline (+EADs: $BVR_{bas} = 3.1 \pm 0.3$ ms vs. $BVR_{dof} = 20.0 \pm 3.9$ ms; $n = 10$; $P = 0.005$, *Figure 5F*). In contrast to what was observed for APD, BVR during dofetilide administration was significantly increased between the two groups, suggesting a better prediction by BVR of pending arrhythmias ($BVR_{dof\text{-}no\ EADs} = 8.3 \pm 1.8$ ms vs. $BVR_{dof\text{-}+EADs} = 20.0 \pm 3.9$ ms; $n = 10$; 10; $P = 0.005$).

Repolarization effects by I_{Kr} block in human-induced pluripotent stem cell-derived cardiomyocytes monolayers

Next, we focused on the response to I_{Kr} block in 2D monolayers of Pluricyte® CMs, using MEA technology. *Figure 6A* shows representative traces of field potentials at baseline and after application of escalating concentrations of dofetilide. The FPD increased progressively, as summarized in *Figure 6B*. Similarly, as for single Pluricyte® CMs, BVR of FPD was evaluated for each concentration. *Figure 6C* shows a representative example of the Poincaré plot for a specific electrode at 0.3, 1, and 3 nmol/L dofetilide. The extreme increase in FPD-BVR at the highest concentration preceded the first arrhythmic event, similar to what was found in isolated hiPSC-CMs. On average, BVR showed a concentration-dependent increase, which was highest at 3 nmol/L (110 ± 25 ms; *Figure 6D*).

At 3 nmol/L, dofetilide caused single abnormal impulses or bursts of arrhythmia in ~30% of the electrodes (in a total of eight wells analysed), whereas at 10 nmol/L 88% of the electrodes showed arrhythmias and the remaining 12% displayed a quiescent signal (*Figure 6E*).[4] Representative examples are depicted in *Figure 6F*.

Discussion

In the present study, we determined the action-potential contour, duration and rate dependence of hiPSC-CMs (Pluricyte® CMs), after setting the resting membrane potential to −85 mV. The ion currents investigated, i.e. I_{Na}, I_{Kr}, I_{CaL}, revealed properties of amplitude, kinetics and voltage dependence similar to other hiPSC-CM lines and, to some extent, to native CMs. Intracellular Ca^{2+}-handling studies showed a functional Ca^{2+}-induced Ca^{2+}-release, a sizable ECC gain, and an adequate response to caffeine. During I_{Kr} block by dofetilide, prolongation of APD_{90} was accompanied by an increased BVR, especially before first EADs occurred. Multi-electrode array experiments on hiPSC-CMs monolayers confirmed this pronounced increase in BVR, actually before the first occurrence of abnormal impulses and bursts of arrhythmia.

The 'I_{K1} injection' achieved by DC enabled us to characterize the AP parameters at a near-physiological resting membrane potential. This is particularly important for the recruitment and functioning of Na^+ channels and for I_{CaL} and I_{Kr}. Analogous to adult native cells, Pluricyte® CMs showed a typical rate dependence in APD. The use of DC did not decrease the cell-to-cell variability in the APD_{90}, as was already shown in ventricular-like hiPSC-CMs by Verkerk *et al.*[8]

The I_{Na} in Pluricyte® CMs showed a robust amplitude and a typical steady-state voltage-dependent activation and inactivation at 70 mmol/L extracellular Na^+ concentration (used to assure proper voltage control). Our I_{Na} data are comparable to results obtained in other hiPSC-CMs cell lines.[6] There are only few reports on I_{Na} in native human CMs and the comparison is difficult because of different experimental conditions. In the report on hiPSC-CMs by Sakakibara *et al.*,[9] both activation and inactivation mid-points were more hyperpolarized than in our hiPSC-CMs. Window I_{Na} was shifted more to the left, with a crossing-point at −70.5 mV, compared to Pluricyte® CMs at −57 mV. The temporal dynamics of I_{Na} inactivation in Pluricyte® CMs were comparable to those of non-diseased native human CMs, as reported by Sakakibara *et al.*,[9] being (at −20 mV) $\tau_F = 2.1 \pm 0.1$ ms and $\tau_S = 12.0 \pm 0.7$ ms. Recently, Goodrow *et al.*[10] analysed I_{Na} differences in ventricular and atrial human CMs, and in a commercially available hiPSC-CM line. These investigators observed

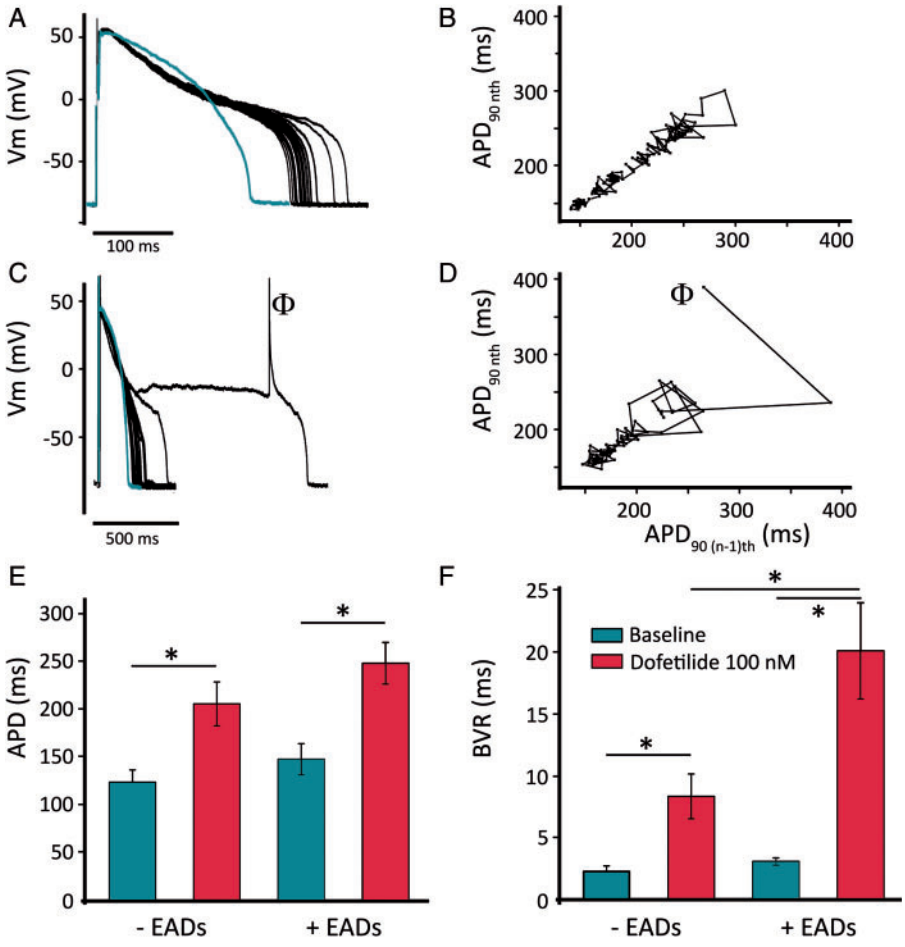

Figure 5 Increased BVR precedes EAD generation. (*A*) Representative example of repolarization variability by I_{Kr} block without EAD generation, compared to baseline (green trace). (*B*) Poincaré plot of APD_{90} of the same cell as in panel (*A*). (*C*) Representative example of repolarization variability by dofetilide, compared to baseline (green trace; note the different time axis), in a cell that eventually generated an EAD (indicated by the symbol Φ). (*D*) Poincaré plot of APD_{90} of the same cell as in panel (*C*) before the very first EAD recorded. (*E*) Average APD in cells that developed EADs ($n = 10$) or did not ($n = 10$). (*F*) Average BVR (prior to first EAD, if any) in cells that developed EADs ($n = 10$) or did not ($n = 10$).

that the activation $V_{1/2}$ was about 5 mV more depolarized in hiPSC-CMs compared to native CMs, which is in line with our findings in Pluricyte® CMs. Overall, the differential results on hiPSC-CMs (including Pluricyte® CMs) vs. human adult native CMs could be explained, at least partly, by a differential expression of β-subunits in these cellular models, able to influence the channel voltage dependency and expression level.[11] Furthermore, Veerman *et al.*[12] showed that hiPSC-CMs express a considerable level of the neonatal isoform of Nav1.5, which decreases progressively with time of cell culture. The adult and neonatal isoforms differ in their voltage dependence,[12] which could also account for differences between hiPSC-CMs and human adult native CMs. Our biophysical characterizations at the single-cell level, together with the MEA data in which the activation amplitude was robust, confirmed the functionality of Na^+ channels in Pluricyte® CMs.

Repolarization in Pluricyte® CMs relied significantly on I_{Kr}, as expected.[6] This is evident from our voltage-clamp recordings, in which I_{Kr} showed a large tail current, almost five times larger than the one reported by Magyar *et al.*[13] in human native cells. This discrepancy may be explained by the methodological issues during native cardiomyocyte isolation, which could cause the loss of ion channels at the membrane. The rectifier ratio curve was useful in estimating the proportion of maximal I_{Kr} conductance functionally expressed during the AP plateau, thus contributing to APD. Considering that I_{Kr} recovery from inactivation is almost instantaneous at −40 mV, the rectifier ratio closely reflects the voltage dependence of channel steady-state inactivation.

The I_{CaL} density measured in Pluricyte® CMs was larger than in human CMs,[14] as already reported in other hiPSC-CM lines,[5] and I_{CaL} window was shifted towards more negative potentials, similar to what was shown by Ma *et al.*[6] Notably, EADs occurred in a range of voltages compatible with the window I_{CaL} measured, which is in line with a role of window I_{CaL} in EAD generation in hiPSC-CMs.

The Ca^{2+}-decay rate in Pluricyte® CMs was similar to that reported by Høydal *et al.*[15] in human native CMs. In our experiments, the recordings of Ca^{2+}-transients were performed at 0.4 Hz to allow

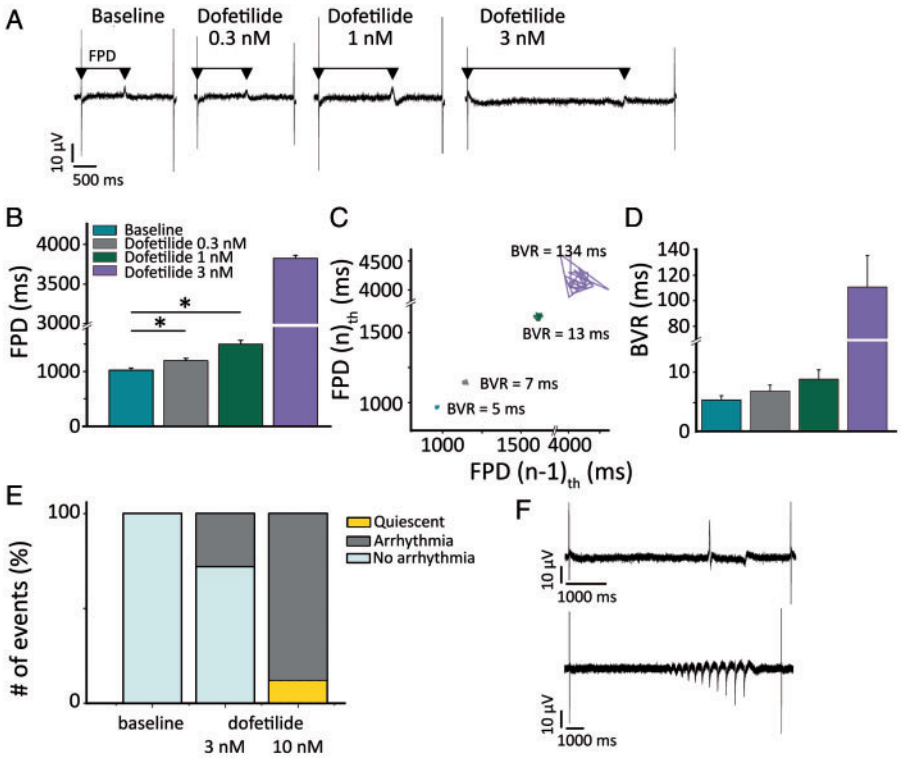

Figure 6 Repolarization instability and arrhythmia in MEAs upon I_{Kr} block. (*A*) Representative field potentials, at escalating dofetilide concentrations (0.3, 1, 3 nmol/L). The arrows indicate the FPD. (*B*) Average values of FPD for each dofetilide concentration ($n = 4$ per condition). (*C*) Poincaré plot depicting the FPD BVR at escalating dofetilide concentration for a selected electrode. (*D*) Average values of FPD BVR in MEAs ($n = 4$). (*E*) Arrhythmia inducibility as percentage of total events, at baseline and during dofetilide 3 and 10 nmol/L ($n = 8$ per condition). (*F*) Representative examples of two types of arrhythmia [single abnormal impulse (above) and burst (below)] triggered by dofetilide.

complete relaxation, which was not achievable at faster frequencies. When we compared the inactivation kinetics of I_{CaL} during the Ca^{2+}-transient recordings, when the intracellular Ca^{2+} was minimally buffered, to those obtained in the voltage-clamp experiments with Ca^{2+} buffered by a high EGTA concentration, we observed a reduction in the τ from 51 ± 4.5 to 37 ± 12 ms, demonstrating the negative-feedback of SR Ca^{2+} release on I_{CaL} (Ca^{2+}-induced inactivation).

The response to caffeine was larger than in other hiPSC-CMs cell lines.[16] The fractional SR Ca^{2+} release calculated for Pluricyte® CMs was 51%, in line with human native CMs (extrapolated from Coppini *et al.*[14] and Høydal *et al.*,[15] both approximatively 45–50%). In hiPSC-CMs, the T-tubular network, which promotes efficient Ca^{2+}-induced Ca^{2+} release, lacks the abundance and detailed organization found in adult CMs. To measure the efficiency of coupling between I_{CaL} and SR Ca^{2+} release, the ECC gain is widely used. Parikh *et al.*[7] described a new protocol to induce the maturation of T-tubules in hiPSC-CMs and reported a lower ECC-gain value than Pluricyte® CMs (at 0 mV, ECC gain of the control hiPSC was 0.03 A.U., and for 'tubulated' cells 0.1 A.U., compared to Pluricyte® CMs of 0.15 A.U.). SERCA contribution to cytosolic Ca^{2+} clearance in Pluricyte® CMs was comparable with adult native CMs, as reported by Hwang *et al.*[5] in rabbit isolated CMs and in different hiPSC-CMs lines (rabbit CM: 63%; hiPSC-CMs 58–63%). Taken together, the data suggest that the Ca^{2+} machinery of Pluricyte® CMs appears relatively similar to native CMs, and it assures a proper contraction (see Supplementary material online, *Table S2* for a detailed comparison between electrophysiological and Ca^{2+}-handling parameters of Pluricyte CMs, other hiPSC-CMs lines and human native CMs).

Drug-induced repolarization prolongation is an important component of proarrhythmic risk assessment. However, multiple literature reports indicate BVR as a better risk marker than prolongation alone.[17] Sala *et al.*[18] demonstrated increased repolarization variability in different hiPSC-CM lines upon the administration of the I_{Kr} blocker astemizole. We assessed the contribution of I_{Kr} to repolarization in Pluricyte® CMs at the AP level by applying dofetilide: this caused a pronounced AP prolongation and EAD generation in half of the cells treated. Furthermore, dofetilide (100 nmol/L) increased BVR significantly. Our data demonstrate that BVR can be used as a proarrhythmic marker in hiPSC-CMs, also when computed I_{K1} is injected through DC. Higher concentrations (than 100 nmol/L) of dofetilide in single Pluricyte® CMs had dramatic effects on repolarization, driving them to a non-reversible plateau arrest.

Interestingly, when we analysed the instability of repolarization in cells that developed EADs vs. those that did not, the increase in BVR from baseline to dofetilide was considerably larger in the +EAD cells. Temporal development of BVR preceded the first EAD, as was already demonstrated in native CMs,[17] as well as in human embryonic stem cell-derived cardiomyocytes subjected to I_{Kr} block.[19] This

endorses the increase of BVR as a precursor of subsequent arrhythmias. BVR also increased (but less so) in cells that eventually did not develop EADs. Interestingly, BVR was significantly larger in cells with eventual EAD generation vs. those without, while APD did not show a statistically significant difference between the two groups. This endorses BVR as a more specific marker of arrhythmia inducibility compared to repolarization prolongation, which is especially relevant given the increasing use of hiPSC-CMs in the fields of safety pharmacology and drug development.

Multi-electrode arrays offer a medium/high throughput platform enabling the recording of extracellular field potentials, which have been correlated with action potentials and, to some extent, to the electrocardiogram, and of particular interest for (medicinal) compound testing.[20] We focused on the effect of I_{Kr} block on FPD, its BVR and the arrhythmia inducibility. As already shown for isolated Pluricyte® CMs, BVR increase was concentration-dependent. At 3 nmol/L concentration of dofetilide, before the first arrhythmic event occurred, BVR had increased by >10 times, suggesting a mechanism similar to that in single hiPSC-CMs. Interestingly, when we analysed the presence of arrhythmia-like events from dofetilide 3 nmol/L to 10 nmol/L, we noticed a pronounced increase in the arrhythmia count (single abnormal impulses/bursts). Thus, also our MEA data suggest that an excessive increase in BVR precedes the first arrhythmic event under these conditions. Multi-electrode arrays have been included in the CiPA platform as one of the approaches to evaluate proarrhythmic risk of medicinal compound. We have now demonstrated that the dynamic changes in repolarization instability can be screened using BVR, e.g. using a medium-throughput technique.

Limitations

In this study, the injection of I_{K1} in Pluricyte CMs® through DC provided a resting membrane potential similar to those of native human CMs, assuring a proper recruitment of Na^+ channels. At this moment, the combination of FP recording with I_{K1} injection is not available, so a direct comparison of results from single hiPSC-CMs and 2D monolayers cannot be made. However, electrotonic coupling of myocytes within the 2D monolayer, as well as electrophysiological maturation, may partly compensate for a difference in resting membrane potential between the two models.

A comparison between the duration of the action and field potentials revealed that mean FPD was significantly longer than APD (at baseline). This could be partially due to the fact that single Pluricyte® CMs were paced at 1 Hz, whereas the monolayers were spontaneously beating at approximately 0.5 Hz. Furthermore, the experimental conditions were different: in fact, the recording solutions (Tyrode solution and Pluricyte® CMs Medium) contained different concentrations of electrolytes. The injection of I_{K1} through DC, only possible at single-cell level, could contribute to the difference as well.

The differential concentration-dependent sensitivity of 2D monolayers and isolated Pluricyte® CMs to dofetilide can be attributed to multiple factors. Besides differences in experimental conditions between the two assays, electrotonic coupling and mechanical junctions in the 2D monolayers could promote electrophysiological maturation of hiPSC-CMs, thus potentially changing the expression, modulation and pharmacological responsiveness of ion channels (including I_{Kr}).

Conclusions

Pluricyte® CMs represent a valuable cellular model with ion-current characteristics and Ca^{2+}-handling properties in various ways similar to human adult native CMs. This renders them suitable for *in- vitro* studies on transmembrane action potentials and field potentials. Repolarization instability upon I_{Kr} block, measured as beat-to-beat variability in both APD_{90} and FPD, is a useful parameter in the proarrhythmic risk assessment of agents with I_{Kr}-blocking effects. Increase in beat-to-beat variability of repolarization may outweigh APD90 prolongation per se as proarrhythmic parameter under these conditions.

Supplementary material

Supplementary material is available at *Europace* online.

Funding

This work was supported by the Netherlands CardioVascular Research Initiative (CVON2012-10 PREDICT) and the Health Foundation Limburg, Maastricht, The Netherlands (to P.G.A.V.).

Conflict of interest: T.d.K. and S.B. are, respectively, employee and co-founder of Ncardia. All other remaining authors have no conflicts of interest to declare.

Data availability

Data generated and analysed in this study are included in the article and supplementary material. There are no additional repositories. Data requests should be addressed to P.G.A.V.

References

1. van Mil A, Balk GM, Neef K, Buikema JW, Asselbergs FW, Wu SM *et al.* Modelling inherited cardiac disease using human induced pluripotent stem cell-derived cardiomyocytes: progress, pitfalls, and potential. *Cardiovasc Res* 2018; **114**:1828–42.
2. Bowes J, Brown AJ, Hamon J, Jarolimek W, Sridhar A, Waldron G *et al.* Reducing safety-related drug attrition: the use of *in vitro* pharmacological profiling. *Nat Rev Drug Discov* 2012;**11**:909–22.
3. Shih HP, Zhang X, Aronov AM. Drug discovery effectiveness from the standpoint of therapeutic mechanisms and indications. *Nat Rev Drug Discov* 2018;**17**:19–33.
4. Blinova K, Dang Q, Millard D, Smith G, Pierson J, Guo L *et al.* International multisite study of human-induced pluripotent stem cell-derived cardiomyocytes for drug proarrhythmic potential assessment. *Cell Rep* 2018;**24**:3582–92.
5. Hwang HS, Kryshtal DO, Feaster TK, Sánchez-Freire V, Zhang J, Kamp TJ *et al.* Comparable calcium handling of human iPSC-derived cardiomyocytes generated by multiple laboratories. *J Mol Cell Cardiol* 2015;**85**:79–88.
6. Ma J, Guo L, Fiene SJ, Anson BD, Ja T, Kamp TJ *et al.* High purity human-induced pluripotent stem cell-derived cardiomyocytes: electrophysiological properties of action potentials and ionic currents. *Am J Physiol Heart Circ Physiol* 2011;**301**: 2006–17.
7. Parikh SS, Blackwell DJ, Gomez-Hurtado N, Frisk M, Wang L, Kim K *et al.* Thyroid and glucocorticoid hormones promote functional t-tubule development in human-induced pluripotent stem cell-derived cardiomyocytes. *Circ Res* 2017; **121**:1323–30.
8. Verkerk AO, Veerman CC, Zegers JG, Mengarelli I, Bezzina CR, Wilders R. Patch-clamp recording from human induced pluripotent stem cell-derived cardiomyocytes: improving action potential characteristics through dynamic clamp. *IJMS* 2017;**18**:1873.
9. Sakakibara Y, Furukawa T, Singer DH, Jia H, Backer CL, Arentzen CE *et al.* Sodium current in isolated human ventricular myocytes. *Am J Physiol* 1993;**265**: H1301–9.
10. Goodrow RJ Jr, Desai S, Treat JA, Panama BK, Desai M, Nesterenko VV *et al.* Biophysical comparison of sodium currents in native cardiac myocytes and human induced pluripotent stem cell-derived cardiomyocytes. *J Pharmacol Toxicol Methods* 2018;**90**:19–30.

11. Moreau A, Mercier A, Thériault O, Boutjdir M, Burger B, Keller DI *et al.* Biophysical, molecular, and pharmacological characterization of voltage-dependent sodium channels from induced pluripotent stem cell-derived cardiomyocytes. *Can J Cardiol* 2017;**33**:269–78.
12. Veerman CC, Mengarelli I, Lodder EM, Kosmidis G, Bellin M, Zhang M *et al.* Switch from fetal to adult SCN5A isoform in human induced pluripotent stem cell-derived cardiomyocytes unmasks the cellular phenotype of a conduction disease-causing mutation. *J Am Heart Assoc* 2017;**6**:e005135.
13. Magyar J, Iost N, Kortvely A, Banyasz T, Virag L, Szigligeti P *et al.* Effects of endothelin-1 on calcium and potassium currents in undiseased human ventricular myocytes. *Pflügers Arch* 2000;**441**:144–9.
14. Coppini R, Ferrantini C, Yao L, Fan P, Del Lungo M, Stillitano F *et al.* Late sodium current inhibition reverses electromechanical dysfunction in human hypertrophic cardiomyopathy. *Circulation* 2013;**127**:575–84.
15. Hoydal MA, Kirkeby-Garstad I, Karevold A, Wiseth R, Haaverstad R, Wahba A *et al.* Human cardiomyocyte calcium handling and transverse tubules in mid-stage of post-myocardial-infarction heart failure. *ESC Heart Fail* 2018;**5**:332–42.
16. Zhang XH, Haviland S, Wei H, Saric T, Fatima A, Hescheler J *et al.* Ca^{2+} signaling in human induced pluripotent stem cell-derived cardiomyocytes (iPS-CM) from normal and catecholaminergic polymorphic ventricular tachycardia (CPVT)-afflicted subjects. *Cell Calcium* 2013;**54**:57–70.
17. Thomsen MB, Verduyn SC, Stengl M, Beekman JD, de Pater G, van Opstal J *et al.* Increased short-term variability of repolarization predicts d-sotalol-induced torsades de pointes in dogs. *Circulation* 2004;**110**:2453–9.
18. Sala L, Yu Z, Ward-van Oostwaard D, van Veldhoven JP, Moretti A, Laugwitz KL *et al.* A new hERG allosteric modulator rescues genetic and drug-induced long-QT syndrome phenotypes in cardiomyocytes from isogenic pairs of patient induced pluripotent stem cells. *EMBO Mol Med* 2016;**8**:1065–81.
19. Nalos L, Varkevisser R, Jonsson MK, Houtman MJ, Beekman JD, van der Nagel R *et al.* Comparison of the ikr blockers moxifloxacin, dofetilide and E-4031 in five screening models of pro-arrhythmia reveals lack of specificity of isolated cardiomyocytes. *Br J Pharmacol* 2012;**165**:467–78.
20. Kim J, Shah D, Potapov I, Latukka J, Aalto-Setälä K, Räsänen E. Scaling and correlation properties of RR and QT intervals at the cellular level. *Sci Rep* 2019;**9**:3651.